Available online at www.sciencedirect.com
ScienceDirect
Polymer 48 (2007) 1343–1351
polymer
www.elsevier.com/locate/polymer

Relationship between segmental dynamics and tracer diffusion of low mass compounds in polyacrylates

Satoshi Maji[1], Osamu Urakawa, Keiichiro Adachi*

Department of Macromolecular Science, Graduate School of Science, Osaka University, 1-1 Machikaneyama, Toyonaka, Osaka 560-0043, Japan

Received 23 June 2006; received in revised form 30 November 2006; accepted 22 December 2006
Available online 27 December 2006

Abstract

We studied the relationship between segmental dynamics of matrix polymers and tracer diffusion of low mass compounds by the use of forced Rayleigh scattering and dielectric spectroscopy. Specifically poly(methyl acrylate), poly(ethyl acrylate) and poly(*n*-butyl acrylate) were used as the polymer matrices and six azobenzene derivatives with various substituents as the diffusant. The temperature dependence of the tracer diffusion coefficient D was measured on methylyellow (MY)/polyacrylate blends at the MY concentration of 1 wt%. The results indicate that the temperature dependence of D is weaker than the dielectric loss maximum frequencies f_m for the α processes of the matrices. The effect of volume of the dye molecules on D was also investigated at 305 K. Comparison of the tracer diffusion coefficients among various dye/polymer systems indicates that $\log D$ in the same matrix decreases linearly with the molar volume of the dyes.

Keywords: Tracer diffusion coefficient; Azobenzene derivatives; Poly(alkyl acrylate)

1. Introduction

Diffusion of low mass compounds in polymer matrices has been studied long [1–25] because of its relevance to various applications such as gas permeation [3], membrane separation [26], ionic conduction [27,28], thin film [24,25] and controlled release of drugs [29]. Those experimental studies revealed that the diffusion coefficient D of low mass compounds above glass transition temperatures T_g is closely related to the segmental dynamics of the matrix polymers [1–3]. So far most of the results of measurements of D were analyzed theoretically on the basis of free volume theories proposed by Fujita [2] and developed by Vrentas and Duda [5,6]. Various modifications of the theory have been proposed for precise prediction of D [14–16]. However, the relationship between D and local segmental dynamics of the matrix polymers has not been studied fully.

In order to explain dynamic and relaxation behaviours of polymers and supercooled liquids near T_g, many researchers assume cooperative segmental dynamics [30–32]. The idea of the cooperative dynamics leads us to expect that components of a mixture obey the same dynamics and therefore the mobility of a low mass compound in a polymer exhibits the same temperature and composition dependences as the segmental dynamics of the polymer chains. Contrary to this expectation, recent studies on miscible polymer blends revealed that the dynamics of components in binary mixed systems are distinct [32–35]. This behaviour is called ‘‘dynamic heterogeneity’’ [34]. Although many studies on diffusion of low mass compounds in polymers have been reported, systematic studies focusing on the relationship between the segmental dynamics and diffusion of low mass compounds are rare [7,13,18–20,36]. Ediger and his coworkers reported the rotational and translational diffusions of probe molecules such as rubrene dissolved in polymers [18–20]. Inoue et al. found that the rotational correlation functions of the probes depend on the size of the probe molecules

* Corresponding author. Tel.: +81 6 6850 5464; fax: +81 6 6848 9265.
E-mail address: adachi@chem.sci.osaka-u.ac.jp (K. Adachi).
[1] Present address: Sumitomo Bakelite Co., Ltd., 2-3-47 Higashi-Tukaguchi, Amagasaki 661-8588, Japan.

0032-3861/$ - see front matter © 2007 Elsevier Ltd. All rights reserved.
doi:10.1016/j.polymer.2006.12.039

and that the temperature dependence of rotational correlation time is similar to the viscoelastic relaxation time of the polymer matrices [36]. Cicerone et al. [19] and Wang and Ediger [20] found that the temperature dependence of the diffusion coefficient of probes is weaker than that of rotational diffusion. Similar results were also reported for the other systems [7,13].

Dynamic heterogeneity is most clearly observed in polymer/diluent systems i.e., the motions of the diluent molecules such as toluene and polymer segments are almost perfectly decoupled [37]. We found that the distribution of the dielectric relaxation times broadens due to concentration fluctuation. The dynamic heterogeneity depends on the size of low mass molecules: we reported the dielectric relaxations of phenyl-, biphenyl- and terphenyl derivatives dissolved in polystyrene and found that dynamic heterogeneity becomes weak with increasing size of the low mass compound [38,39]. Tracer diffusion of probes in glass forming low mass compounds such as *o*-terphenyl was also reported and similar behaviours to probe/polymer systems were observed [40–42].

We aim to examine the dynamic heterogeneity in polymers containing low mass compounds focusing on the tracer diffusion and dielectric segmental relaxation of the matrix polymers. For this purpose we have carried out measurements of forced Rayleigh scattering (FRS) [9,10,13,40,41,43,44] and dielectric relaxation on poly(methyl acrylate) (PMA), poly(ethyl acrylate) (PEA) and poly(butyl acrylate) (PBA) containing a trace amount of azobenzene derivatives (dyes) in temperatures above T_g of these polymers. There are two objectives. Firstly we compare the temperature dependences of the dielectric relaxation frequency (loss maximum frequency f_m) of the matrix polymers and the diffusion coefficient D of the dyes dissolved in the matrices. The dynamic heterogeneity observed in dye/polyacrylate systems will be discussed by testing the time–temperature superposability. As mentioned above the size of low mass molecules plays an important role in local dynamics. The second objective is to examine the effect of the molar volume of dye molecules on D. The results will be discussed on the basis of molecular models including the free volume theory.

2. Experimental

2.1. Materials

Poly(methyl acrylate) (PMA), poly(ethyl acrylate) (PEA) and poly(butyl acrylate) (PBA) were purchased from Aldrich (USA). The molecular weights of PMA, PEA and PBA were 40, 99 and 95 kg/mol, respectively and the glass transition temperatures of PMA, PEA and PBA were 283, 248 and 219 K, respectively. Various dyes having the structure of $C_6H_5{-}N{=}N{-}C_6H_4{-}R$ were used where R denotes a group attached at the *para* position with respect to the azo-group. Azobenzene (AB), 4-phenylazobenzoylchloride and methylyellow (MY) were purchased from Aldrich (USA). Azobenzene derivatives with the ester groups were synthesized from 4-phenylazobenzoylchloride and alcohols or phenols: $C_6H_5{-}N{=}N{-}C_6H_4{-}COCl + R'OH \rightarrow C_6H_5{-}N{=}N{-}C_6H_4{-}COOR' + HCl$. The code and structures of these dyes are summarized in Table 1.

Table 1
Structures and van der Waals volumes V of dyes[a]

Dyes[b]	Code	Structure of R	V/nm^3
Azobenzene	AB	$-H$	0.139
Methylyellow	MY	$-N(CH_3)_2$	0.176
p-Carbopentoxy-ABz	C5	$-COOC_5H_{11}$	0.223
p-Carbododecoxy-ABz	C12	$-COOC_{12}H_{25}$	0.306
p-Carbo(3-methylphenoxy)-ABz	CR	$-COOC_6H_4CH_3$	0.235
p-Carbobiphenoxy-ABz	BP	$-COOC_6H_4{-}C_6H_5$	0.281

[a] Van der Waals volumes V were calculated by assuming the additivity of the group volumes [45].
[b] ABz is abbreviation of azobenzene.

For the sake of later discussion, the van der Waals volumes of the dyes were calculated by assuming the additivity of the group volumes [45] and listed in Table 1.

The samples for FRS measurements were prepared by casting chloroform solutions (ca 20 wt%) of a polymer and a dye on a piece of slide glass. The solvent was removed completely under vacuum of 0.01 Pa at 350 K for 3 days. The cast film on the glass plate was sandwiched with another glass plate and compressed on a hot-press machine at about 370 K. The thickness of the sample was adjusted to be 150 μm with spacers. The content of the dyes was mostly 1 wt% but for the MY/PMA system, the content was changed from 1 to 15 wt% to examine the effect of the dye content.

2.2. Methods

Measurements of the tracer diffusion coefficient of the dyes were made by using a homemade apparatus of forced Rayleigh scattering (FRS) [43,44]. The writing and reading beams were Ar ($\lambda = 488$ nm, ca. 0.2 W) and He–Ne ($\lambda = 633$ nm, 3 mW) beams, respectively. The scattering angle was from 2.5° to 15° corresponding to the Bragg spacing from 7.3 to 1.2 μm. The intensity of the scattered light was detected with a photomultiplier tube (Hamamatsu Photonics Co., C1550-04, Hamamatsu, Japan). The signal was amplified by a homemade differential amplifier to compensate the coherent noise (see Eqs. (3) and (4)). The compensation voltage was precisely adjusted so that the output voltage became zero before the exposure to the writing beam. The amplified signal was recorded in a personal computer equipped with an A/D converter. A typical example of the signal is shown in Fig. 1.

Glass transition temperature T_g was determined by a differential scanning calorimeter (Seiko Instruments & Electronics Ltd., DSC-20, Japan) at 10 K/min. T_g was determined as the middle point of the stepwise change of the DSC thermograms. Dielectric measurements were performed by using two RLC meters (QuadTech, models 1693 and 7600, USA).

2.3. Analyses of FRS data

In FRS measurements, a sample polymer containing a dye is exposed by two coherent writing beams with the same intensity $I_0/2$ but with different incident angles for a short period of the order of 1 s [43,44]. The interference of the two beams

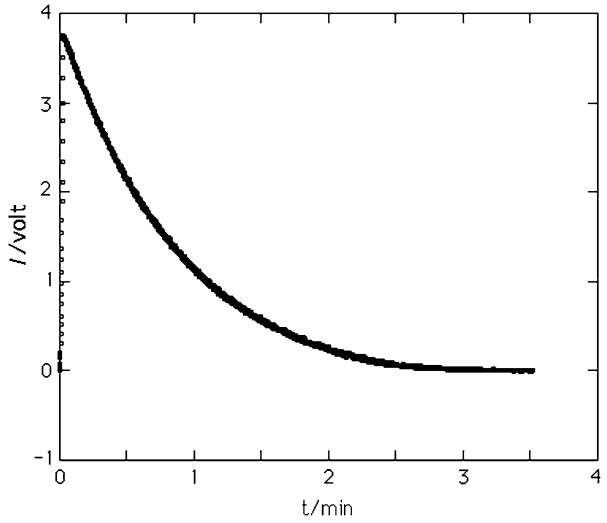

Fig. 1. An example of the time dependence of scattered light for NY/PEA at 315 K.

causes a sinusoidal change of the intensity of the light being proportional to $\cos^2(\pi x/d)$. Here d is the wavelength of the interference fringe and x is the coordinate along which the fringe is formed. The dye molecules isomerize in proportion to the intensity of the writing beam forming a sinusoidal change of the refractive index. Then the fringe causes scattering of a reading beam in the direction where the Bragg condition is fulfilled. The concentrations of the non-isomerized molecules ϕ_1 and isomerized ones ϕ_2 are given by

$$\phi_1 = \phi_0 - \phi_2 \tag{1}$$

$$\phi_2 = \xi\phi_0 I_0 \cos^2(\pi x/d) \tag{2}$$

where ϕ_0 is the total concentration of the dye molecules and ξ the coefficient of isomerization. The amplitude of thus created fringe decreases with time by the diffusion of the dye molecules and hence the intensity $I(t)$ of scattered light decreases with time t:

$$I(t) = k[\alpha\exp(-t/\tau_1) - \beta\exp(-t/\tau_2) + \gamma]^2 \tag{3}$$

where k, α and β are the constants and γ the coherent noise mainly due to the light scattered at the surface of the sample cell and colloidal dusts which have not been removed by a filter with the smallest mesh size of 0.2 μm. τ_1 and τ_2 are the time constants due to the diffusion of the non-isomerized (1) and isomerized (2) molecules, respectively. If the diffusion coefficients D_1 and D_2 of the non-isomerized and isomerized molecules differ, the decay curve becomes superposition of the four exponential functions with the time constants τ_1, τ_2, $2\tau_1$ and $2\tau_2$ [44]. In the present experiments, we controlled the experimental condition so that γ was much larger than α and β. Thus the terms of α^2, β^2 and $\alpha\beta$ are smaller than the first order terms and hence $I(t)$ can be written as

$$I(t) \cong \alpha'\exp(-t/\tau_1) - \beta'\exp(-t/\tau_2) + I_\infty \tag{4}$$

where $\alpha' = 2k\alpha\gamma$, $\beta' = 2k\beta\gamma$ and I_∞ is the base line equal to γ^2. The time constants τ_1 and τ_2 are given by

$$\frac{1}{\tau_j} = \frac{16\pi^2 D_j}{\lambda^2}\sin^2(\theta/2) + \frac{1}{\tau_{\text{dye}}} \tag{5}$$

where $j = 1$ or 2, λ the wavelength of the reading beam and τ_{dye} is the time constant for thermal isomerization of the dye. Depending on the values of α/β and τ_1/τ_2, the time dependence of $I(t)$ exhibits different profiles as given by Eq. (4) [44]. In the present study, $I(t)$ decreased monotonously conforming to the single exponential decay curve as shown in Fig. 1. Thus we were not able to determine τ_1 and τ_2 separately. The origin of the monotonous decay curve is that τ_1 for the *trans*-isomer (the stable form) is close to τ_2 for the *cis*-isomer. Thus Eq. (4) is rewritten as

$$I(t) \cong I_0\exp(-t/\tau) + I_\infty \tag{6}$$

The example of the $1/\tau$ versus $\sin^2(\theta/2)$ is shown in Fig. 2. The values of the tracer diffusion coefficient of the dyes are determined from the slope of such plots.

3. Results and discussion

3.1. Dielectric relaxation

Fig. 3 shows the temperature dependences of the dielectric loss factor ε'' at 1 kHz for pure PMA, PEA and PBA. The main loss peaks locate about 30 K above the glass transition temperatures T_g of each polymer and are assigned to the α relaxation due to segmental dynamics. Broad loss peaks due to the β relaxation are also seen in the temperature range below T_g. The dielectric relaxations of PMA [46,47], PEA [46] and PBA [48]

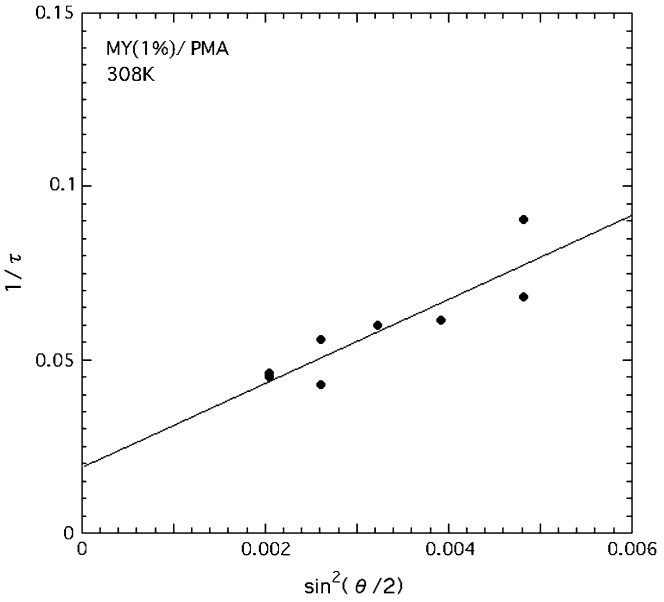

Fig. 2. Example of the plot of $1/\tau$ (s^{-1}) against $\sin^2(\theta/2)$.

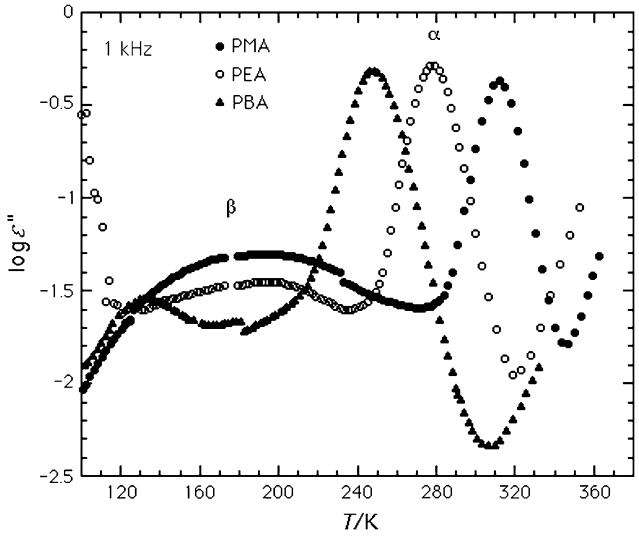

Fig. 3. The temperature dependence of $\log \varepsilon''$ of pure PMA, PEA and PBA.

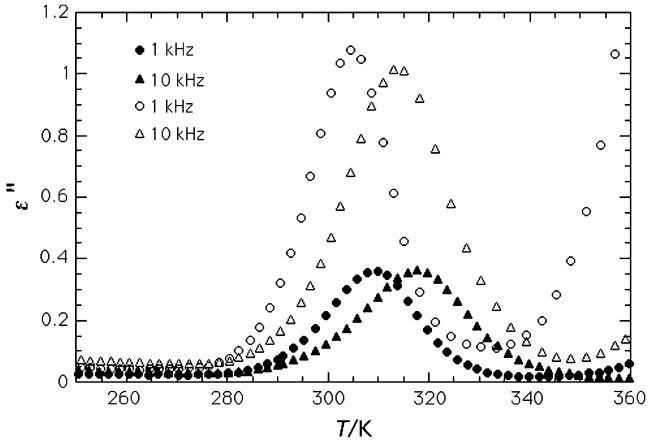

Fig. 4. Comparison of ε'' curves at 1 and 10 kHz between pure PMA (closed keys) and PMA containing 15 wt% MY (open keys).

were already reported. The present data approximately agree with those previous data.

Fig. 4 compares the temperature dependences of ε'' of pure PMA and those of the MY/PMA mixture containing 15 wt% of MY. Measurements were carried out after quenching the sample from ca 400 to 200 K. It is seen that the α peak of PMA containing 15% MY locates at temperatures ca 15 K lower than that of pure PMA at 1 kHz due to the plasticizing effect of MY. If the MY molecules reorient at a different rate from that of the PMA segments, the mixture would exhibit two loss peaks due to the components. In Fig. 4 it is seen that the ε'' curves for the MY (15%)/PMA system do not exhibit bimodal loss peaks and that the ε'' peak for the MY/PMA system is about two times higher than that for pure PMA. This indicates that the MY molecules having the high dipole moment of 9.2×10^{-30} C m reorient at the same rate as the PMA segments. Recently we reported that the dielectric α loss peak in polystyrene (PS) containing cyanobenzene (CNBz), alkylcyanobiphenyl (CNBP) and alkyl-cyano-*p*-terphenyl (CNTP) [38,39]. The loss curves for the CNBz/PS and CNBP/PS systems are bimodal due to dynamic heterogeneity, but in the CNTP/PS system, the loss curve becomes unimodal indicating that the terphenyl molecules move cooperatively with the PS segments [39]. The MY/PMA system exhibits behaviour similar to the CNTP/PS system suggesting cooperative motions of the MY molecules and the PMA segments. Although we did not carry out dielectric measurements on the MY/PEA and MY/PBA blends, we expect that behaviours in those systems are similar to those in the MY/PMA system. However, this view of cooperative motions is not harmony with the data of tracer diffusion of the MY molecules as discussed later.

3.2. Diffusion of MY and segmental dynamics in PMA, PEA and PBA

The temperature dependences of the diffusion coefficient D of MY in PMA, PEA and PBA were measured at the MY content of 1 wt% and plotted in Fig. 5a–c, respectively. The loss maximum frequency f_m for the dielectric α processes of pure PMA PEA and PBA are also plotted for the sake of comparison. The data of f_m are fitted to the Vogel–Fulcher (VF) equation [49,50] and the best fit curves are indicated by the dotted lines:

$$\log f_m = A - \frac{B}{T - T_0} \tag{7}$$

where A and B are constants and T_0 is the critical temperature. The parameters A, B and T_0 are listed in Table 2. The parameter B for PBA differs significantly from that reported previously [48]. The origin of the discrepancy is not clear. In Fig. 5, we see that the tracer diffusion coefficients at a fixed temperature increase with decreasing T_g of the polymer matrix as expected. It is seen that in the MY/PMA system, the temperature dependences of D and f_m are different, but in the MY/PEA and MY/PBA systems, $\log D$ changes almost parallel to the VF equation for $\log f_m$.

Let us discuss these results. We note that measurements of D in the MY/PMA system were made near T_g, namely in the range of $10\ \mathrm{K} < T - T_g < 50\ \mathrm{K}$, but in the MY/PEA and MY/PBA systems measurements were made in the range $T - T_g > 40$ K. Since it is known generally that dynamic heterogeneity in mixed systems is enhanced with approaching T_g, the distinct behaviours among the systems can be explained as the result of such a general trend. In fact we see in Fig. 5 that the temperature dependence of D and f_m in the MY/PMA system tends to become similar in the high-temperature region.

From these results one may expect that the temperature dependence of D is expressed as a function of T_g/T or $T - T_g$. Fig. 6 shows the plots of $\log D$ versus $T - T_g$. It is seen that the data of $\log D$ of different systems do not conform to a common curve as indicated by the solid lines. The plots of $\log D$ versus T/T_g exhibit similar behaviours to Fig. 6. We expect that the temperature dependence of D is a function of the parameters of the VF equation, since Brownian motions of the dye molecules take place as a result of thermal agitation by

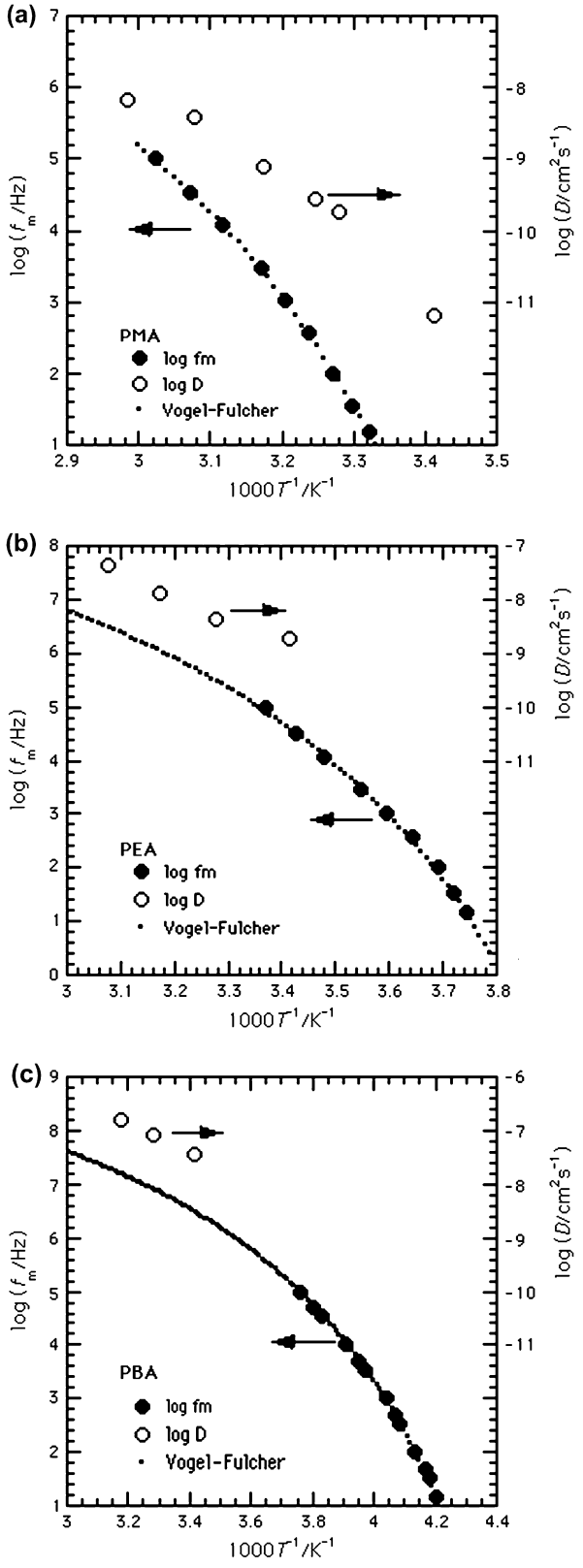

Fig. 5. Comparison of the temperature dependence of the tracer diffusion coefficient D of MY (open circle) and the dielectric loss maximum frequency f_m of matrices (closed circle) in MY/PMA (a), MY/PEA (b) and MY/PBA (c). The dotted lines indicate the VF equation with the parameters listed in Table 2.

Table 2
Parameters of the Vogel–Fulcher equation for the segmental relaxation of PMA, PEA and PBA

	A	B	T_0
PMA	11.2	488	252.6
PEA	10.6	425	222.2
PBA	10.2	341	200.0

segmental motions of the matrix polymer. Therefore we attempted to express the diffusion coefficient as a function of T, A, B and T_0. Among various attempts, we found that the plots of $\log D - A$ and $\log f_m - A$ with respect to $B/(T - T_0)$ conform, respectively, to common curves as shown in Fig. 7. Since the temperature ranges of measurements of D in the MY/PEA and MY/PBA systems are narrow, the data of more wide temperature range are required to confirm the superposability of the data of the $\log D - A$ versus $B/(T - T_0)$ plot. Here we discuss the diffusion behaviour of MY assuming this superposability as is often assumed in measurements of viscoelasticity.

The plot of $\log D - A$ versus $B/(T - T_0)$ does not conform to a straight line in contrast to $\log f_m - A$. This indicates the dynamic heterogeneity between the diffusion of the MY molecules and the segmental dynamics of matrix polymers. However, the fact that $\log D$ can be expressed by a function of the VF parameters indicates the close relationship between diffusion and segmental dynamics. We have sought a function of temperature to which $\log D - A$ becomes linear and found that the plots of $\log D - A$ versus $[1/(T - T_0)]^{1/2}$ conform to a straight line as shown in the inset of Fig. 7. Therefore the T-dependence of D is approximately given by

$$\log D = A + K_1 - \frac{K_2 B^{1/2}}{\sqrt{T - T_0}} \tag{8}$$

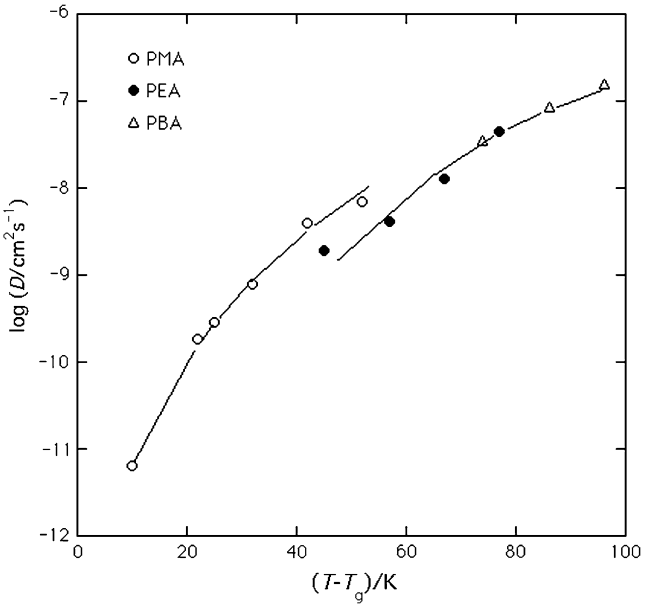

Fig. 6. Plots of $\log D$ (cm^2 s^{-1}) against $T - T_g$ (K) for the MY/PMA, MY/PEA and MY/PBA systems. The solid lines are guide for the eyes.

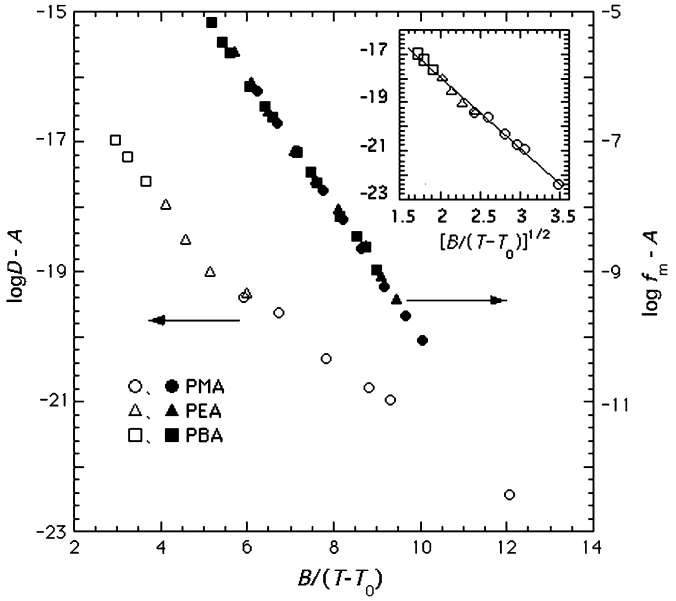

Fig. 7. Plots of $[\log(D/\mathrm{cm^2\,s^{-1}}) - A]$ and $[\log(f_m/\mathrm{Hz}) - A]$ against $B/(T - T_0)$ for MY/PMA, MY/PEA and MY/PBA where A, B and T_0 are the parameters of the VF equation and are listed in Table 2.

where K_1 and K_2 are constants equal to -11.65 and 3.10, respectively. We have also found that the tracer diffusion coefficients in the methylacetate/PMA system [7], tetracene/polystyrene (PS) and rubrene/PS [19] conform to Eq. (8) with the dielectric data of PS [46]. The value of K_2 for the methylacetate/PMA system is close to 3.1 but those of the latter two systems are higher than that of the present system. The parameter A of the VF equation represents the relaxation frequency at infinitely high temperature and corresponds to the average frequency of thermal vibration. The above-mentioned results indicate that the diffusion of low mass molecules is sensitive to such vibration as well as T_0 and B.

The dielectric data shown in Fig. 4 have indicated that the rotational relaxation times of the MY molecules and the PMA segments are almost the same. In contrast, the results shown in Fig. 7 and Eq. (8) indicate that the diffusion and the segmental dynamics obey distinct dynamics, namely they are dynamically heterogeneous. The weaker temperature dependence of D than f_m means that the tracer diffusion occurs faster than the segmental motions at low temperatures near T_g. This is demonstrated by calculating the mean square displacement $\langle R^2 \rangle$ of the MY molecule in the period τ $(= 1/(2\pi f_m))$ needed for reorientation of the polymer segment. For the MY/PMA system, τ is 0.016 s and $\langle R^2 \rangle^{1/2}$ becomes 25 nm at 300 K. This value is much longer than the length of the MY molecule of 1.6 nm: the distance of the migration of the MY molecules during one rotation of the PMA segment is ca 16 times of the size of the MY molecule. The value of $\langle R^2 \rangle^{1/2}/\tau$ increases with decreasing temperature. These puzzling observations may be explained as follows.

The present results are similar to those studied by Cicerone et al. [19,42] for probes of tetracene and rubrene in polystyrene (PS): i.e., the temperature dependence of diffusion of the probe molecules is weaker than that of rotation. Cicerone et al. explained the results by assuming a spatially heterogeneous distribution of free volume which causes mobile and immobile regions in PS [19]. They explained that the observed rotational correlation function of the probe is a weighted average of the correlation function for the probes locating different regions and hence the correlation time for the reorientation is heavily influenced by the slowest motion, but the translational Brownian motions of probe molecules tend to occur through mobile regions. Ediger wrote a review on this problem [18]. The present results may be explained in terms of their model. However, no direct evidences of the heterogeneous structure have been observed by scattering methods. We also note that this model predicts that the dielectric relaxation spectra in pure amorphous polymers broaden significantly with decreasing temperature but such behaviour has not been reported for typical amorphous polymers such as poly(vinylacetate) [46].

The other explanation may be possible by considering anisotropic diffusion of the MY molecules in polymer matrices, i.e., the mobility in the direction of the long axis is higher than that in the perpendicular direction. In dielectric measurements, the overall reorientation of the long axis of the MY molecules is observed as the direction of the dipole moment coincides with that of the long axis. Since the length of the long axis (1.6 nm) of the MY molecule is similar to the average size of the units of segmental dynamics (1–2 nm), rotational motions of the MY molecules are hindered by the PMA chains and hence the relaxation time for reorientation of the MY molecules becomes similar to that for segmental motions. On the other hand, translational motions of the MY molecules in polymer matrices occur mainly in the direction of the long axis of the MY molecules. In this case we expect that the size of the short axis of the MY molecules governs effectively the diffusion process and hence the MY molecules migrate a long distance during τ for segmental motions of PMA. We need to investigate the tracer diffusion for low mass compounds with various aspect ratios to confirm the anisotropic diffusion.

3.3. Effect of volume of dye molecules on diffusion coefficient

In this section we examine the effect of the van der Waals volume V of the dyes on D of the dyes. We have calculated V assuming the additivity of the atomic volumes and are listed in Table 1 [45]. Fig. 8 shows the plots of $\log D$ versus V at 305 K dissolved in PMA, PEA and PBA. The content of dyes was 1 wt%. Fujita et al. reported the diffusion coefficients of methyl-, ethyl-, propyl- and butylacetate in PMA [7]. Their data at 305 K are extrapolated to zero concentration and plotted in Fig. 8. Although the data points are scattered, $\log D$ increases with decreasing V and the $\log D$ versus V curves are approximately linear:

$$\log D = C_1 - C_2 V \tag{9}$$

where C_1 and C_2 are constants depending on T. At 305 K, C_2 is approximately equal to $-6.6 \pm 1.1\ \mathrm{nm^{-1}}$ for all systems and C_1 for PMA, PEA and PBA systems are -7.6 ± 0.5,

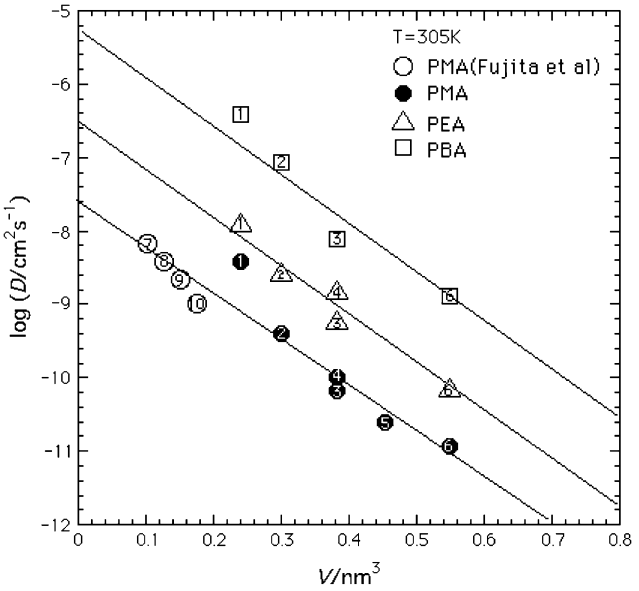

Fig. 8. Plots of $\log D$ ($cm^2\ s^{-1}$) versus the molar volume V (nm^3) of the dye molecules listed in Table 1. The circle, triangle and square keys represent the polymer matrices of PMA, PEA and PBA, respectively. The indices indicated in the keys represent the diffusants, i.e., 1, AB; 2, MY; 3, C5; 4, CR; 5, BP; 6, C12; 7, CH_3COOCH_3; 8, $CH_3COOC_2H_5$; 9, $CH_3COOC_3H_7$; 10, $CH_3COOC_4H_9$. The data of the indices 7–10 in open circles are those reported by Fujita et al. [7].

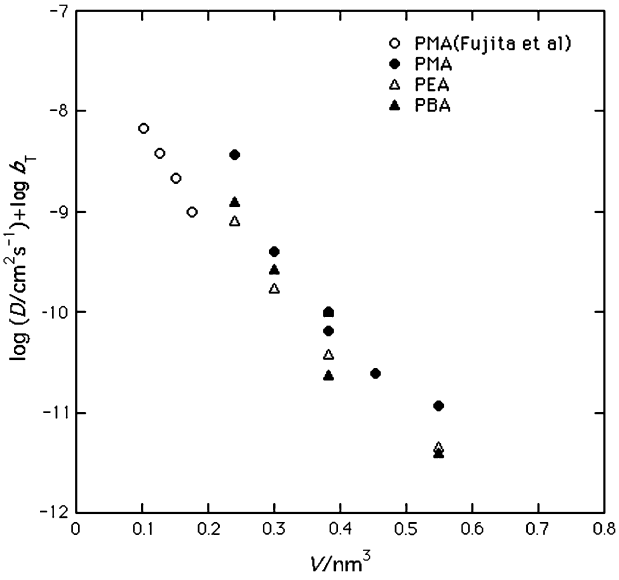

Fig. 9. Master curve of $\log D$ ($cm^2\ s^{-1}$) versus V (nm^3) of dye molecules in PMA, PEA and PBA at 305 K where the friction for the dye molecules is reduced to that in PMA matrix. The data in PEA and PBA are shifted by −1.0 and −2.2 decades along the ordinate, respectively.

-6.5 ± 0.5 and -5.2 ± 0.5, respectively. Relatively large scatter of the data points indicates that the diffusion of the dyes depends on the specific shapes and intermolecular interactions of the dye molecules as well as V. It is seen that the present data and the data reported by Fujita et al. [7] conform approximately to the same straight line despite the large difference of molecular structure.

The Stokes law predicts for a spherical particle with radius a that its diffusion coefficient is proportional to the inverse of a. Therefore if the classical fluid dynamics holds for diffusion of the dyes, the $\log D$ versus $\log V$ plot has the slope of $-1/3$. Although not shown here, the plots of $\log D$ versus $\log V$ for the present systems are curved and the average slopes are as high as -5.5 ± 1.5. Von Meerwall et al. studied diffusion of n-alkanes in rubbers and that of plasticizers in poly(vinyl chloride) [51,52]. They determined D at zero concentration of the low mass compounds by extrapolation of the data of D. In Ref. [51], they reported that D was proportional to M^{β} with β ranging from -0.7 to -1 depending on the polymer matrices (SB rubber and PI) where M is the molecular weight of the alkanes. This dependence is higher than $-1/3$ but is lower than our result if V is assumed to be proportional to M. However in Ref. [52], they reported that there was no correlation between D and M. The V dependence of D will be discussed on the basis of the free volume theory in the later section.

We attempted to superpose the $\log D$ versus V curves by taking the dye/PMA system as the reference state. Fig. 9 shows the master curve in which the data of $\log D$ of the dyes in PEA and PBA are shifted by -1.1 and -2.4 decades, respectively. The plots are scattered largely indicating that D depends mainly on V but also depends on the specific molecular structure of the dye and specific intermolecular interactions between the dye and the polymer matrix. The shift factors b obtained above represent the ratio of the friction ζ for the diffusion process of the dye molecules in the different polymer matrices: for example $\log b$ for the dye/PEA system is equal to $\log[\zeta(\text{PEA})/\zeta(\text{PMA})]$. On the other hand, the friction for the segmental dynamics is proportional to f_m^{-1}. From the Arrhenius plots shown in Fig. 5, the shift factors of f_m^{-1} between the PMA and PEA and between PMA and PBA become -3.2 and -5.1 decades, respectively, which are quite different from $\log b$ for the tracer diffusion of the dyes. This again indicates the dynamic heterogeneity between the tracer diffusion of dyes and the segmental dynamics of matrix polymers.

We see in Fig. 8 that the data of the diffusion coefficients of alkylacetates in PMA reported by Fujita et al. [7] conform to the same straight line for the dyes. If the dynamic heterogeneity depends on the size of the diffusants, the plots of $\log D$ versus V would exhibit a break at some value of V. Unfortunately the scatter of data is relatively large and we cannot find such a cross-over point in Fig. 8.

We again discuss the average displacement $\langle R^2 \rangle^{1/2}$ of the low mass molecules during the period τ ($= 1/(2\pi f_m)$) for reorientation of the polymer segment. From the relation of $\langle R^2 \rangle = 6D\tau$ and Eq. (9), $\langle R^2 \rangle^{1/2}$ at 305 K is written by a form:

$$\langle R^2 \rangle^{1/2} = \kappa \times 10^{-C_2 V/2} \tag{10}$$

where κ is constant and V the van der Waals volume in nm^3. The values of κ at 305 K for the matrices of PMA, PEA and PBA are calculated to be 175, 10.1 and 8.2 nm, respectively. This equation indicates that $\langle R^2 \rangle^{1/2}$ of a low mass molecule in PMA at 305 K is much longer than the segment size but

$\langle R^2 \rangle^{1/2}$ in PBA is similar to the segment size. For example the benzene molecule having the volume of 0.117 nm^3 migrates 72 nm in the period of τ of PMA at 305 K, but in the PBA matrix it migrates 3.4 nm which is similar to the size of the segment. Thus Eq. (10) indicates that the dynamic heterogeneity is enhanced with decreasing $T - T_g$. It is expected that Eq. (10) holds in a certain range of V since the Stokes law holds for a large diffusant.

3.4. Comparison with free volume theory

Vrentas and Duda proposed the theory of D of low mass compounds in polymer matrices based on a free volume theory [5,6]. At the limit of zero content of a low mass compound, D is given by

$$D = D_0 \exp\left(-\frac{E^*}{RT} - \frac{\gamma V_p^0(0)\xi}{V_{HF}} \right) \tag{11}$$

where D_0 is constant, E^* the activation energy needed to overcome the attractive forces of the surrounding molecules, γ the dimensionless overlapping factor, $V_p^0(0)$ the specific volume of the polymer at 0 K and V_{HF} the hole free volume of the polymer per 1 g at T and ξ the ratio of the critical volume V_{lmc}^* for jump of the low mass compound and that V_p^* of the jumping unit of the polymer. So far many authors tested this equation for mixtures of polymers and ordinary solvents such as benzene [3].

Firstly we discuss the temperature dependence of D based on Eq. (11). The second term in the exponent of Eq. (11) has a form similar to the Doolittle equation [53]. Duda et al. expressed the viscosity η of the polymer using the parameters included in Eq. (11) [54]:

$$\log \eta = C + \frac{0.434\gamma V_p(0)}{V_{HF}} \tag{12}$$

where C is the constant. The T-dependence of $\log \eta$ can be expressed by the VF equation: $\log \eta = A' + B/(T - T_0)$ where A' is the constant. Then Eq. (11) is rewritten to a form:

$$\log D = C' - \frac{0.434E^*}{RT} - \frac{\xi B}{T - T_0} \tag{13}$$

where C' is equal to $\log D_0 - \xi(A' - C)$. In order to use this equation, we need to evaluate E^* and $\xi = V_{lmc}^*/V_p^*$. The data of E^* and ξ are not available for the MY/polyacrylate systems. We roughly estimate ξ as follows.

Zielinski and Duda proposed an empirical equation: $V_p^* = 0.6224T_g - 87$ cm^3/mol [55]. From this equation we estimate V_p^* of PMA, PEA and PBA to be 89, 67 and 49 cm^3/mol, respectively. For a rigid molecule, the free volume model assumes that V_{lmc}^* is equal to the van der Waals volume V of the molecule. Vrentas et al. defined $\xi_L = V/V_p^*$ and proposed a theory on the effect of the asymmetrical structure of diffusant molecules on ξ [16]. According to their theory, ξ of an asymmetrical molecule is less than ξ_L by a factor of $\psi = 1/\{1 + \xi_L(1 - Y/X)\}$ where X/Y is the aspect ratio of the molecule. The molar volume V of MY is estimated to be 181 cm^3/mol as given in Table 1 and the values of ξ_L for MY/PMA, MY/PEA and MY/PBA systems become 1.9, 2.7 and 3.7, respectively. It is difficult to evaluate the aspect ratio of the MY molecule as it has a complex structure. We roughly estimate that $X/Y = 2.4$ for the *trans*-MY and $X/Y = 1.0$ for *cis*-MY molecule from the stereo structure of the MY molecule. Here we assumed that $X/Y = 1.09$ for the benzene ring as given in Ref. [16]. Thus we obtain $\xi = \xi_L$ for the *cis*-MY/polyacrylate systems. The values of ξ for *trans*-MY/polyacrylate systems become 0.90, 1.3 and 1.8 for the matrices of PMA, PEA and PBA, respectively.

Thus evaluated ξ values indicate that the third term of Eq. (13) has a temperature dependence similar to or stronger than $\log f_m$. The second term $-E^*/T$ further enhances the T-dependence of $\log D$. Therefore Eq. (11) predicts a stronger temperature dependence of $\log D$ than $\log f_m$. However, the experimental results shown in Fig. 7 indicate that the T-dependence of $\log f_m$ is much stronger than that of $\log D$. Therefore the present experimental results cannot be explained by the free volume theory.

Secondly the dependence of D on V is discussed. It is known that E^* depends on combinations of polymer and diffusant [16]. We tentatively assume that E^* is independent of the structures of the dyes used in this experiment. Then Eq. (11) predicts that $\log D$ is proportional to $\psi\xi$. If we further assume that the values of ψ of the dyes are similar, $\log D$ is expected to be proportional to $-V$. In Fig. 8 we see that Eq. (11) holds roughly. However, as already pointed out in Section 3.3 the scatter of the data points in Fig. 8 is large. This may be attributed to the difference of E^* and ψ of the dyes in the framework of the free volume theory. It is noted that among the dyes used in this experiments, AB, MY, CR and BP have rigid structure but the alkyl groups of C5 and C12 are flexible. For flexible molecules V_{lmc}^* should be equal to the volume of the jumping unit and therefore the assumption of $V_{lmc}^* = V$ does not hold for C5 and C12. Nevertheless we see in Figs. 8 and 9, that the data points of these dyes locate approximately on the same straight lines and hence the flexibility does not affect much the tracer diffusion coefficient of the dyes.

In this section we have analyzed the experimental results using the free volume theory. To summarize the temperature dependence of D of MY in polyacrylates cannot be explained by the free volume theory. But the V dependence of D of the dyes is approximately explained.

4. Conclusion

We measured the tracer diffusion coefficient D of azobenzene derivatives (dyes) in PMA, PEA and PBA and the dielectric relaxation frequencies f_m for the α processes of the matrix polymers. The temperature dependence of the tracer diffusion coefficient D of methylyellow (MY) was measured at the MY concentration of 1 wt%. The dependence of D on the van der Waals volume V was examined for azobenzene derivatives. We

found that the temperature dependence of D is weaker than f_m indicating that the dynamics of the dye molecules and segmental motions are dynamically heterogeneous. However, the dielectric loss curve of PMA containing 15 wt% of MY is unimodal indicating that reorientation of the MY molecules and segmental motions are apparently dynamically homogeneous. This puzzling result may be explained either by the spatially heterogeneous structure proposed by Ediger et al. [18,19] or by the anisotropic diffusion of the MY molecules. The values of $\log D - A$ in the MY/PMA, MY/PEA and MY/PBA systems are found to be linear against $-[B/(T-T_0)]^{1/2}$ and conform to a common straight line where A, B and T_0 are the parameters of the Vogel–Fulcher equation for f_m of the matrix polymers.

The data of D of various dyes at 305 K indicate that $\log D$ in the same matrix polymer is approximately linear with respect to the van der Waals volume V of the dyes. The slopes of the $\log D$ versus V plots in PMA, PEA and PBA are approximately the same and a master curve has been constructed by shifting the data of the PEA and PBA systems by -1.1 and -2.4 decades, respectively. Those shift factors are much smaller than the ratio of f_m of the matrices. The average displacement $\langle R^2 \rangle^{1/2}$ of the dye molecules during the period τ $(= 1/(2\pi f_m))$ for reorientation of the polymer segment is calculated. $\langle R^2 \rangle^{1/2}$ in PMA is found to be much longer than the size of the dye molecule but in PBA the value is similar to the size of the dye molecule. The results indicate that the dynamic heterogeneity is enhanced with approaching T_g. Those results have been compared with the free volume theory. The temperature dependence of D of MY in polyacrylates cannot be explained by the free volume theory. But the V dependence of D of the dyes is approximately in agreement with the free volume theory.

References

[1] Crank J, Park GS. Diffusion in polymers. New York: Academic Press; 1968.
[2] Fujita H. Fortschr Hochpolym Forsch 1961;3:1.
[3] Klopffer MH, Flaconneche B. Oil Gas Sci Technol Rev IFP 2001;56:223.
[4] Cohen MH, Turnbull D. J Chem Phys 1959;31:1164.
[5] Vrentas JS, Duda JL. J Polym Sci Polym Phys Ed 1977;15:403.
[6] Vrentas JS, Duda JL. J Appl Polym Sci 1978;22:2325.
[7] Fujita H, Kishimoto A, Matsumoto K. Trans Faraday Soc 1960;56:424.
[8] Pace RJ, Datyner A. J Polym Sci Polym Phys 1979;17:437, 453, 465.
[9] Wang CH, Xia JL. J Chem Phys 1990;92:2603.
[10] Wang CH, Xia JL, Yu BK. Macromolecules 1991;24:3638.
[11] Arnould D, Laurence RL. Ind Eng Chem Res 1992;31:218.
[12] Waggoner RA, Blum FD, Macelroy JMD. Macromolecules 1993;26:6841.
[13] Ehlich D, Sillescu H. Macromolecules 1990;23:1600.
[14] Hong SU. Ind Eng Chem Res 1995;34:2536.
[15] Hong SU. J Appl Polym Sci 1996;61:833.
[16] Vrentas JS, Vrentas CM, Faridi N. Macromolecules 1996;29:3272.
[17] Deppe DD, Dhinojawala A, Torkelson JM. Macromolecules 1996;29:3898.
[18] Ediger MD. Annu Rev Phys Chem 2000;51:99.
[19] Cicerone MT, Blackburn FR, Ediger MD. Macromolecules 1995;28:8224.
[20] Wang CY, Ediger MD. Macromolecules 1997;30:4770.
[21] Song Y, Srinivasarao M, Tonelli A, NcGregor R. Macromolecules 2000;33:4478.
[22] Tonge MP, Gillbert RG. Polymer 2001;41:501.
[23] Tonge MP, Stubbs JM, Sundberg DC, Gillbert RG. Polymer 2001;41:3659.
[24] Tseng KC, Turro NJ, Durning CJ. Phys Rev E 2000;61:1800.
[25] Pu Y, White H, Rafailovich MH, Sokolov J, Patel A, White C, et al. Macromolecules 2001;34:8518.
[26] Greenfield ML, Theodorou DN. Macromolecules 1998;31:7068.
[27] Subbarao EC. Solid electrolyte and their application. New York: Plenum; 1980.
[28] Mitani K, Adachi K. J Polym Sci B Polym Phys 1995;33:947.
[29] Narasimhan B, Peppas NA. J Pharm Sci 1997;86:297.
[30] Adam G, Gibbs JH. J Chem Phys 1965;43:139.
[31] Adachi K. Macromolecules 1990;23:1816.
[32] Matsuoka S, Quan X. Macromolecules 1991;24:2770.
[33] Alegria A, Colmenero J, Ngai KL, Roland CM. Macromolecules 1994;27:4486.
[34] Lodge TP, McLeish TCB. Macromolecules 2000;33:5278.
[35] Hirose Y, Urakawa O, Adachi K. Macromolecules 2003;36:3699 and references cited therein.
[36] Inoue T, Cicerone MT, Ediger MD. Macromolecules 1995;28:3425; Adachi K, Fujihara I, Ishida Y. J Polym Sci Polym Phys Ed 1975;13:2155.
[37] Nakazawa M, Urakawa O, Adachi K. Macromolecules 2000;33:7898.
[38] Hori H, Urakawa O, Adachi K. Polym J 2003;35:721.
[39] Urakawa O, Ohta E, Hori H, Adachi K. J Polym Sci Polym Phys Ed 2006;44:967.
[40] Heuberger G, Sillescu H. J Phys Chem 1996;100:15255.
[41] Fujara F, Geil B, Sillescu H, Fleischer G. Z Phys B 1992;88:195.
[42] Cicerone MT, Ediger MD. J Chem Phys 1996;104:7210.
[43] Hervet H, Urbach W, Rondelez F. J Chem Phys 1978;68:2725.
[44] Spiegel DR, Sprinkle MB, Cang T. J Chem Phys 1996;104:4920.
[45] Haward RN. J Macromol Sci Rev Macromol Chem 1964;C4:441.
[46] McCrum NG, Read BE, Williams G. An elastic and dielectric effects in polymeric solids. New York: John Wiley & Sons; 1967 and Dover Publications Inc: New York; 1991.
[47] Ishida Y. Kolloid-Z 1961;174:124.
[48] Hayakawa T, Adachi K. Polymer J 2000;32:845.
[49] Vogel H. Phys Z 1921;22:645.
[50] Fulcher JG. J Am Ceram Soc 1925;8:339.
[51] Von Meerwall E, Ferguson RD. J Appl Polym Sci 1979;23:3657.
[52] Von Meerwall E, Skowronski D, Harihara A. Macromolecules 1991;24:2441.
[53] Doolittle AK. J Appl Phys 1951;22:1471.
[54] Duda JL, Vrentas JS, Ju ST, Lin HT. AIChE J 1982;28:279.
[55] Zielinski JM, Duda JL. AIChE J 1992;38:405.